Oxadiazole Derivatives As Promising Anti Breast Cancer Agents: A Computational Study Of Molecular Docking And Pharmacokinetic Parameters

Rekha S[1], Ajay Karabhari[2], Ajay Kumar R[3], Supritha K M[4], Thejesh H M[5], S Ashwath Narayan[6], Vinod C K[7], Jyothi V B[8]

[1]Department of Pharmaceutical Chemistry, College of Pharmaceutical Sciences, Dayananda Sagar University, Bangalore, India

[2,3,4,5,6,7,8]Research Scholar UG, College of Pharmaceutical Sciences, Dayananda Sagar University, Bangalore, India

Abstract: Cancer continues to be one of the foremost causes of death globally, influenced by a combination of genetic and environmental elements. In women, breast cancer is among the most prevalent and lethal types. This study investigated the anti-breast cancer properties of oxadiazole derivatives.

4, 5-disubstituted 1, 3, 4-Oxadiazole derivatives were synthesized and evaluated for their anti-breast cancer effects on VEGFR-2, using the protein 3VHK. The ADME and drug-likeness assessments demonstrated that all compounds exhibit favorable pharmacokinetic characteristics.

All the compounds showed a strong affinity for the enzyme. The new derivatives were authenticated through FT-IR, 1 H-NMR, and LCMS analyses. Each of the derivatives displayed impressive docking scores between -8.6 and -9.5, which were assessed against the reference standard lenvatinib, which had a docking score of -7.7.

In vitro experiments were conducted to further explore the lead candidate's effectiveness against MCF-7 cell lines, with a positive control of lenvatinib. Nearly all derivatives exhibited more encouraging activity against the VEGFR enzyme.

Keywords: Oxadiazoles, VEGFR, Molecular docking, Druglikeness, MCF-7 cell lines, Anti-breast cancer activity.

INTRODUCTION

One of the most deadly illnesses in the world is cancer, caused by a combination of environmental and hereditary factors, including diet. The leading cause of cancer-related death in women is breast. To increase the survival time of individuals with breast cancer, new options for treatment are required 1.Oxadiazoles are five membered heterocyclic rings containing nitrogen (two atoms) and oxygen (one atom). Derivatives of 4, 5-disubstituted 1, 3, 4-oxadiazoles represents a fascinating class of compounds, which have garnered interest in medicinal chemistry as bioisosteres for various biological targets 2. Due to these properties, 1,3,4-oxadiazole derivatives have shown a wide range of biological activities, including antimicrobial3, anti-HIV4, antitubercular5, anticonvulsant6, anti-inflammatory7, analgesic8, antiviral8, as well as uses in pesticides8, insecticides and anthelminthic10 applications.In metastasis, angiogenesis—the creation of new blood vessels from preexisting vasculature—is essential. Growth factors control this process, and VEGF (vascular endothelial growth factor) is a major player due to its influence on the activity of vascular smooth muscle cells (VSMC) and endothelial cells (EC) 11, 12. Six isoforms of the VEGF gene are produced by alternative splicing, with VEGF-A being the most physiologically active. Neuropilin (NRP; NRP1 and NRP2), a nontyrosine kinase, and two receptor tyrosine kinases, VEGFR-1 and VEGFR-2, are bound by VEGF-A. But the main receptor that VEGF uses to control angiogenesis and endothelial function is VEGFR-2. When VEGFR-2 is bound, a tyrosine kinase signaling cascade is started, which encourages cell proliferation and survival, migration, and differentiation into mature blood vessels, as well as vasodilatation through nitric oxide (NO) and prostacyclins13, 14.Lenvatinib is a multi-targeted tyrosine kinase inhibitor (TKI) that has gained interest because of its potential application in breast cancer treatment. This is primarily due to its inhibition of VEGFRs (Vascular Endothelial Growth Factor Receptor), which play a crucial role in tumor angiogenesis15.In this study, we sought to determine the suitability and likelihood of new techniques for synthesizing 4, 5-disubstituted-1, 3, 4-oxadiazole derivatives. Molecular docking and ADME serves as quick and effective computational approaches to anticipate the optimal alignment of bioactive substances with a specific protein 16

Drugs & Chemicals: All the chemicals were procured from Sigma-Aldrich. The compounds used were highest analytical grade.

Protein data bank (PDB)

PDB is a database containing three-dimensional structural information for large biological molecules, including proteins and nucleic acids. The majority of the structures are established through X-ray diffraction and NMR examinations. Every structure released in the PDB is assigned a four-character alphanumeric code known as a PDB ID, for example, 3VHK[17].

Molecular docking

Docking studies were performed to examine the various biomolecular interactions and the binding affinities between ligands and receptors. Molecular docking is performed using Autodock vina. The protein structure in three dimensions is obtained from the protein data bank (PDB ID- 3VHK). Autodock Vina is an open-source application that includes a comprehensive molecular viewer and graphical tools for conducting molecular docking. PyMOL generates a high-quality 3D representation of proteins along with their visualization. PyRx is intended for docking analysis [18]. The docking analysis was carried out on the PPARG Nuclear protein (PDB ID: 3VHK). The computational tasks were conducted on a HP 15s-eq0132au Laptop equipped with an AMD Ryzen 7 3700U processor.

Protein preparation

The VEGF-signaling pathway is the key regulator of tumor growth and metastasis and preparation of this enzyme for docking to see the affinity of nova designed molecules. Crystal structure of the VEGFR2 kinase domain in complex with a back pocket binder structure is retrieved from protein data bank (PDB) that is 3VHK with resolution of 2.49 Å.

In this study, rigid docking is executed. The initial binding site on 6HF3 is anticipated using a program named CASTp 3.0 (Computational Atlas of Surface Topology of proteins), which relies on the latest theoretical and algorithmic findings in computational geometry.

The co-crystallized ligand and drug are also eliminated; the water molecule that could hinder the docking procedure is also excised. Include kollman charges; the chosen protein has (3.264) and is stored in PDBQT format. Next, supplementary steps involve incorporating polar contacts to determine the types of interactions between amino acids during ligand-receptor binding[19]. The prepared protein is shown in (Figure 1).

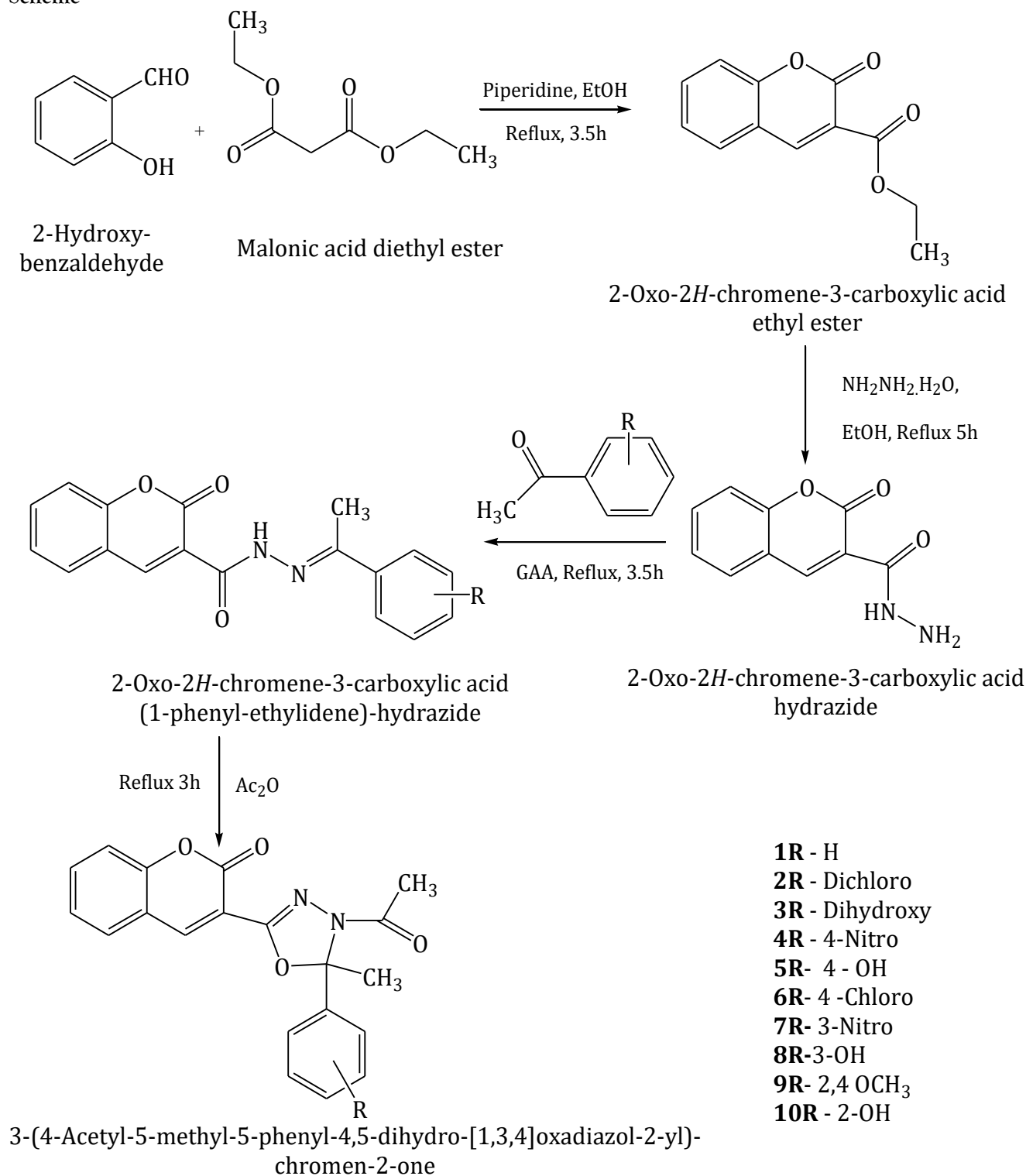**Fig1: 3D** Structure of protein VEGFR (3VHK)
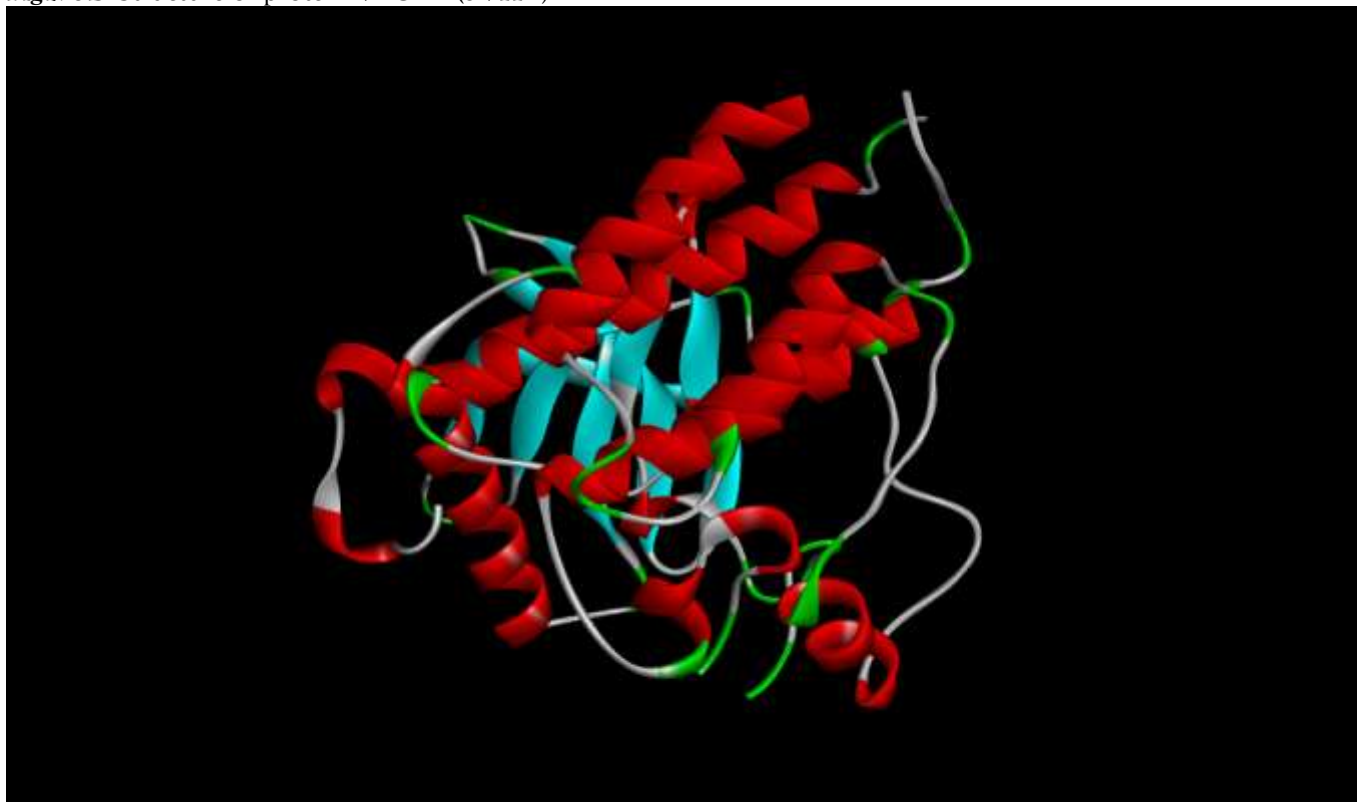
Ligand Preparation

The 2D chemical structures of ligands are drawn using ACD Lab Chemsketch version 12.0 and generated smiles notation. The 3D structures of the ligands were downloaded from RCSB PDB (https://www.rcsb.org) and uploaded

in BIOVIA Discovery Studio Visualizer-2020. Ligand minimization was done and using small molecule wizard in 'SMALL MOLECULE' wizard in BIOVIA Discovery Studio Visualizer-2020 and was saved as a cluster sdf file [20].

Preparation of cell lines [21]

MCF7 human breast adenocarcinoma cell line was used. Cells were obtained from National Centre for Cell Science, Pune, India with 10% FBS and 1% penicillin-streptomycin (Sigma-Aldrich) in a humidified atmosphere with 5% CO2 at 37°C. Cell viability was assessed by MTT assay. The absorbance was measured at 540 nm using a BMGLABTECH-FLUO Star Omega microplate reader (BMG Labtech, Ortenberg, Germany).
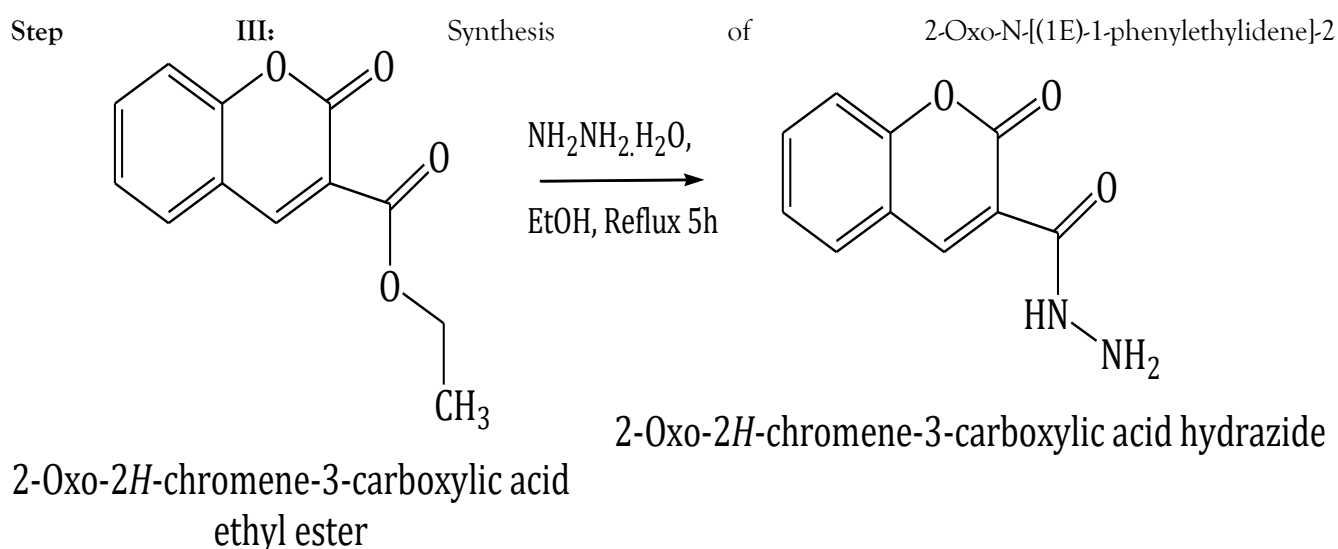
Scheme

2-Hydroxy-benzaldehyde

Malonic acid diethyl ester

Piperidine, EtOH
Reflux, 3.5h

2-Oxo-2*H*-chromene-3-carboxylic acid ethyl ester

$NH_2NH_2.H_2O$,
EtOH, Reflux 5h

2-Oxo-2*H*-chromene-3-carboxylic acid hydrazide

GAA, Reflux, 3.5h

2-Oxo-2*H*-chromene-3-carboxylic acid (1-phenyl-ethylidene)-hydrazide

Reflux 3h | Ac_2O

3-(4-Acetyl-5-methyl-5-phenyl-4,5-dihydro-[1,3,4]oxadiazol-2-yl)-chromen-2-one

1R - H
2R - Dichloro
3R - Dihydroxy
4R - 4-Nitro
5R- 4 - OH
6R- 4 -Chloro
7R- 3-Nitro
8R-3-OH
9R- 2,4 OCH_3
10R - 2-OH

Step I: Synthesis of Ethyl-2-oxo-2H-chromene-3-carboxylate[22]

In a 500-ml RBF equipped with a reflux condenser mixture of salicylaldehyde (0.50 mole) and diethyl malonate (0.55mole) was placed in 100 ml absolute ethanol. To this mixture 2.5 ml of piperidine was added as a catalyst and few drops of glacial acetic acid, and the solution was heated under reflux for 3 hours 20 minutes. The product crystallized readily as the solution cooled and was finally stored overnight in a refrigerator. The crystalline product was collected by filtration and washed with a solution made from 95% ethanol and water (4:6). The crude product was dried in the air and recrystallized from ethanol to give white crystals.


2-Hydroxy-benzaldehyde   Malonic acid diethyl ester   2-Oxo-2*H*-chromene-3-carboxylic acid ethyl ester
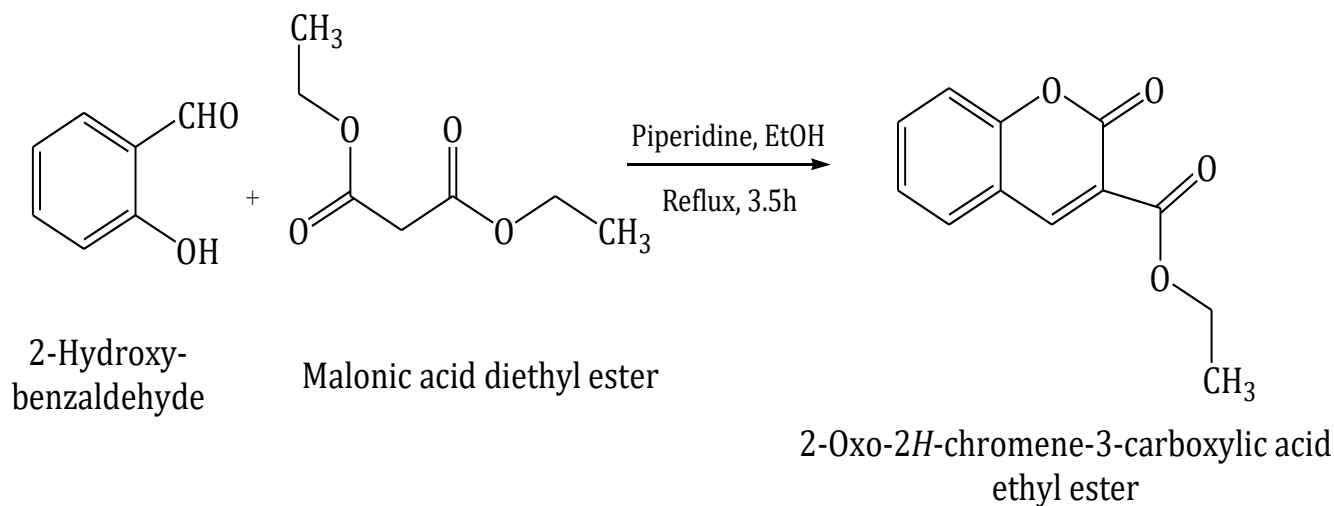
Step II: Synthesis of 2-Oxo-2H-chromene-3-carbohydrazide[23]

A mixture of 0.1 mol of ester and 0.2 mol of hydrazine hydrate were refluxed in 50ml of 95% ethanol for 5-6 hours. The resultant mixture was concentrated, cooled and poured onto crushed ice. The solid mass thus separated out was filtered, dried and purified by recrystallization from ethanol.

Step III: Synthesis of 2-Oxo-N-[(1E)-1-phenylethylidene]-2

2-Oxo-2*H*-chromene-3-carboxylic acid ethyl ester   2-Oxo-2*H*-chromene-3-carboxylic acid hydrazide

H-chromene-3- carbohydrazide [24]

Equimolar amount of 2-oxo-2H-chromene-3-carbohydrazide and aldehydes were dissolved in ethanol and refluxed on water bath for 5-6 hours in presence of few drops of acetic acid. The reaction mixture was poured into ice-cold water and solid was filtered out. The dried solid was recrystallized from ethanol.
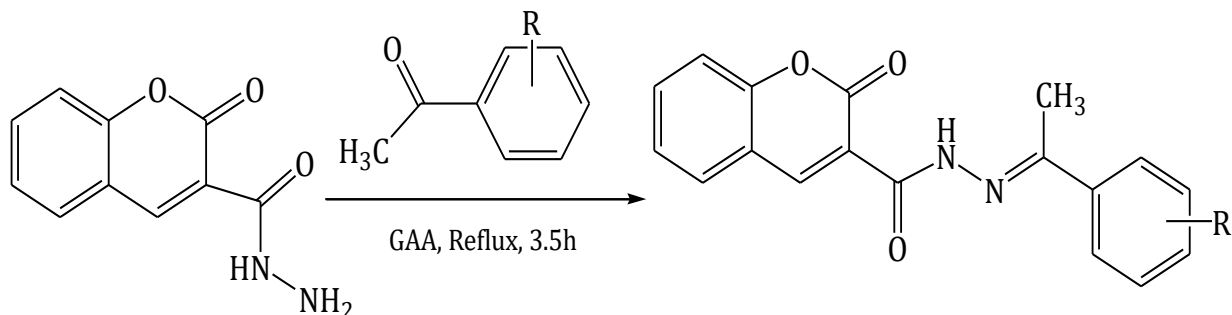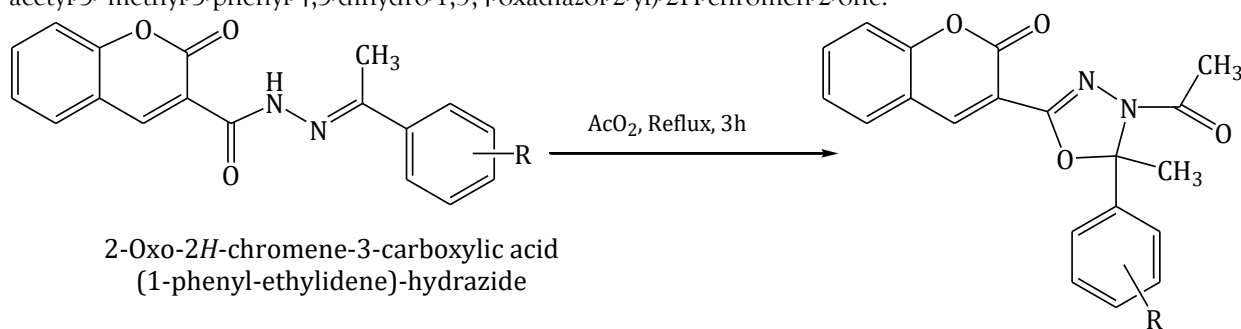
2-Oxo-2*H*-chromene-3-carboxylic acid hydrazide

2-Oxo-2*H*-chromene-3-carboxylic acid (1-phenyl-ethylidene)-hydrazide

Step IV: Synthesis of 3-(4-acetyl-5H-5-phenyl-4,5-dihydro-1,3,4-oxadiazol-2-yl)- 2H-chromen-2-one[25]
A mixture of 2-oxo-N-[(1E)-1-phenylethylidene]-2H-chromene-3-carbohydrazide (0.002 mol) and excess of acetic anhydride (10 mL) was refluxed for 3 hours. The excess acetic anhydride was distilled off at reduced pressure and residue was poured into ice cool water. The solid product was filtered and recrystallized from ethanol to give 3-(4-acetyl-5- methyl-5-phenyl-4,5-dihydro-1,3,4-oxadiazol-2-yl)-2H-chromen-2-one.

2-Oxo-2*H*-chromene-3-carboxylic acid (1-phenyl-ethylidene)-hydrazide
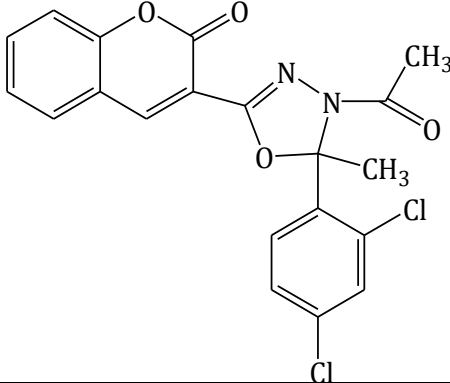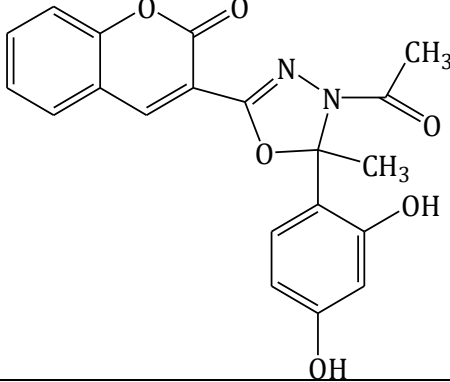
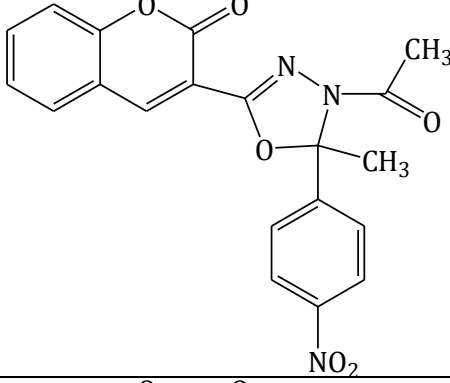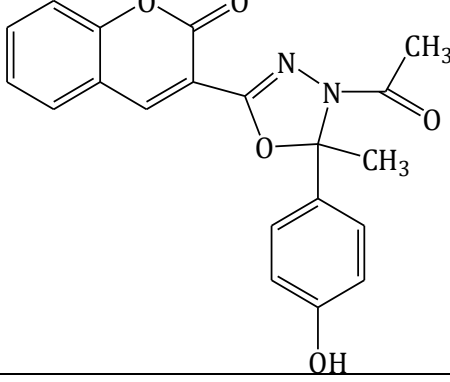3-(4-acetyl-5H-5-phenyl-4,5-dihydro-1,3,4-oxadiazol-2-yl)- 2H-chromen-2-one

1R H, **2R** Dichloro, **3R** Dihydroxy, **4R** 4NO$_2$, **5R** 4OH, **6R** 4-Cl, **7R** 3-NO$_2$, **8R** 3-OH, **9R** 2,4 OCH$_3$,

10R 2OH

Table 1: List of synthesized compounds

Sl.no	Comp code	Chemical name	Structure
1	1R	3-(4-Acetyl-5H-5-phenyl-4,5-dihydro-1,3,4-oxadiazol-2-yl)-2H-chromen-2-one	

2	2R	3-[4-Acetyl-5-(2,4-dichloro-phenyl)-5-methyl-4,5-dihydro-[1,3,4]oxadiazol-2-yl]-chromen-2-one	
3	3R	3-[4-Acetyl-5-(2,4-dihydroxy-phenyl)-5-methyl-4,5-dihydro-[1,3,4]oxadiazol-2-yl]-chromen-2-one	
4	4R	3-[4-Acetyl-5-methyl-5-(4-nitro-phenyl)-4,5-dihydro-[1,3,4]oxadiazol-2-yl]-chromen-2-one	
5	5R	3-[4-Acetyl-5-(4-hydroxy-phenyl)-5-methyl-4,5-dihydro-[1,3,4]oxadiazol-2-yl]-chromen-2-one	

6	6R	3-[4-Acetyl-5-(4-chloro-phenyl)-5-methyl-4,5-dihydro-[1,3,4]oxadiazol-2-yl]-chromen-2-one	
7	7R	3-[4-Acetyl-5-methyl-5-(3-nitro-phenyl)-4,5-dihydro-[1,3,4]oxadiazol-2-yl]-chromen-2-one	
8	8R	3-[4-Acetyl-5-(3-hydroxy-phenyl)-5-methyl-4,5-dihydro-[1,3,4]oxadiazol-2-yl]-chromen-2-one	
9	9R	3-[4-Acetyl-5-(2,4-dimethoxy-phenyl)-5-methyl-4,5-dihydro-[1,3,4]oxadiazol-2-yl]-chromen-2-one	
10	10R	3-[4-Acetyl-5-(2-hydroxy-phenyl)-5-methyl-4,5-dihydro-[1,3,4]oxadiazol-2-yl]-chromen-2-one	

In Vitro Screening for Anti Breast Cancer Activity

Cell Culture [26]

The human breast cancer cell line MCF-7 was obtained from Cells was obtained from National Centre for Cell Science, Pune, India. Cells were cultured in Dulbecco's Modified Eagle Medium (DMEM; Sigma-Aldrich), supplemented with 10% (v/v) Fetal Bovine Serum and 1% (v/v) Penicillin-Streptomycin. Cultures were maintained at 37 °C in a humidified atmosphere containing 5% CO_2 and 95% relative humidity until reaching approximately 80% confluency.

MTT Assay[27]

To evaluate the chemotherapeutic effect of **2R, 4R & 7R** on MCF-7 cell viability, the MTT assay was conducted following previously established protocols. Briefly, cells were seeded in 96-well tissue culture plates at a density of 4×10^4 cells/well and incubated for 48 h at 37 °C. Following incubation, cells were treated with derivatives, lenvatinib (positive control), or dimethyl sulfoxide (DMSO; negative control) for an additional 48 h.

Post-treatment, the culture medium was removed, and MTT solution (0.5 mg/mL) was added to each well and incubated for 2 h at 37 °C in a CO_2 incubator. Supernatant was then removed and DMSO was added to dissolve the MTT formazan. Finally, the absorbance of developed purple color was read at 570 nm using a microplate reader. The cytotoxicity values were evaluated using absorbance values implementing formula:

% Cytotoxicity = $(A_{control} - A_{sample}) / (A_{control})$ x 100

Where, A_{sample} is the absorbance of sample and $A_{control}$ is the absorbance of control.

The half-maximal inhibitory concentration (IC_{50}) was determined from dose-response curves to quantify the efficacy of 1, 3, 4-Oxadiazole derivatives in reducing cell viability.

Statistical Analysis

Cell viability data were obtained from four independent experiments. Statistical analyses were conducted using Graph Pad Prism version 7. A two-way ANOVA followed by Dunnett's post hoc test was employed to assess statistical significance relative to the control group. Data are presented as mean ± standard error of the mean (SEM). Statistical significance was denoted as follows: $p < 0.05$ (), $p < 0.01$ (), **$p < 0.001$** (), and $p < 0.0001$ (****). "N.S." indicates results that were not statistically significant.

In-silico ADME/Pharmacokinetic Predictions[28]

The antagonistic interaction of inhibitors with enzymes or protein receptors alone does not ensure their suitability as potential drug candidates. Therefore, the evaluation of ADME (Absorption, Distribution, Metabolism, and Excretion) properties, along with drug-likeness analysis, plays a crucial role in drug discovery. These assessments support rational decision-making regarding whether an inhibitor can be administered safely and effectively in a biological system. Notably, poor ADME profiles and high toxicity are common reasons for drug failure in the clinical trial phase.

Pfizer's Rule of Five—also known as the Rule of Five (Ro5) or Lipinski's Rule of Five—proposed by Christopher A. Lipinski in 1997, serves as a widely accepted guideline for evaluating drug-likeness. This rule helps determine whether a compound with specific biological and pharmacological characteristics is likely to be orally active in humans. According to the rule, a molecule is considered likely to have good oral bioavailability if it does not violate more than one of the following criteria:

Molecular weight (Mw) < 500

Octanol / water partition coefficient (I LOGP) ≤ 5

Number of hydrogen bond acceptors (nHBA) ≤ 10

Number of hydrogen bond donors (nHBD) ≤ 5

Topological polar surface area (TPSA) < 140 Å²

Based on the ADME and drug-likeness data presented in Table 1, eight molecules exhibited zero violations of Lipinski's Rule, suggesting their strong potential as orally active drugs. These drug-likeness parameters are closely associated with aqueous solubility and intestinal permeability, which are essential for the initial step of oral bioavailability.

Additionally, the results indicated favorable pharmacokinetic properties across all tested molecules, including high gastrointestinal (GI) absorption. None of the compounds were identified as substrates of P-glycoprotein, which often contributes to drug efflux and reduced intracellular concentration. Furthermore, compounds 1A and 5A demonstrated the ability to permeate the blood–brain barrier (BBB), indicating their potential for central nervous system (CNS) activity.

RESULTS AND DISCUSSION

Every derivative prepared during present investigation has been verified using a variety of spectroscopic techniques. Salicyaldehyde was treated with diethyl malonate and a few drops of glacial acetic acid using piperidine as a catalyst and ethanol as a solvent to create the chemical ethyl-2-oxo-2H-chromene-3-carboxylate. The typical peak of the IR spectra was seen at 3059 cm-1 due to Ar C-H str, 1768 cm-1 due to C=O, lactone, 1608 cm-1 due to C=O, ester, 1201 cm-1 due to C-O, coumarin, and 783 cm-1 due to Ar CH bent. The compounds' conformation was further determined by 1HNMR. 8.53 (1H, s, Ar-H), 7.27-7.69 (4H, m, Ar-H), 4.44 (2H, q, CH2), and 1.42 (3H, t, CH3) were obtained when signals were present at δ. 2-oxo-2H-chromene-3-carbohydrazide is obtained by treating this compound with hydrazine hydrate. The formation of this compound is indicated by peaks at 3381cm-1, 3286cm-1, 3037cm-1, 1691cm-1C=O, lactone peak, 1616cm-1 C=O, ketone, 1196cm-1C-O, coumarin, and 750cm-1 Ar CH bend peak. Aldehyde, ethanol, and a few drops of glacial acetic acid are then used to obtain carbohydrazide derivatives, i.e. 2-Oxo-N-[(1E)-1-phenylethylidene]. The IR peaks are used to identify -2H-chromene-3-carbohydrazide. Carbohydrazide derivatives are treated with acetic anhydride to create the substituted 1, 3, 4 oxadiazole derivatives. The oxadiazole nucleus causes 3055 cm-1 Ar-CH str, 1681cm-1C=O, lactone, 1618cm-1C=O, ketone, 1572cm-1C=N, and 1267 cm-1C-O-C. 752 cm-1Ar CH bend, 1195 cm-1 C-O, and coumarin (Table 4). Following purification by column chromatography and confirmation by 1H NMR with signals at δ 2.38 (3H, s, COCH3), 7.32-7.53 (4H, m, Ar-H), 7.8 (2H, d, Ar-H), 8.11 (2H, d, Ar-H), 8.6 (1H, s, Ar-H), and 8.7 (1H, s, CH of oxadiazole), our goal was to truly isolate this chemical (Table 5). By substituting R on the benzene moiety with various electron-donating and electron-withdrawing groups, a number of derivatives were created. In chemical experiment data, a positive sign denotes a good drug, a negative sign denotes a bad drug, and vice versa. Docking postures 2R, 4R, and 7R compounds share five common interactions, and their docking scores were nearly identical to the standard reference lenvatinib, which is -7.7 (Table 6). A well-known VEGFR inhibitor (common medication), lenvatinib interacts with the receptor's active pocket (PDBID: 3VHK) to create three (3) H-bonds with Glu-885, Asp-1046, and His-1026. As illustrated in Figure 2-4, the hydrophobic interactions of chromene with the three amino acid residues Glu-885, Asp-1046, and Arg-1027 in the target's active pocket that lack a hydrogen bond are π-alkyl, alkyl. However, the molecule's 1, 3, and 4 oxadiazole ring moiety and the delocalized π-electron of the benzene ring also interact to create another hydrophobic contact with the Lys 868 amino acid residue.

In vitro anti-breast cancer activity was evaluated using the MTT assay on MCF-7 cell lines**.** Compounds that showed the best docking scores 2R, 4R and 7R with scores -9.5, -9.2 and -9.2 respectively were selected for cytotoxic evaluation against the reference drug Lenvatinib with score -7.7. In addition, the MTT assay results for compounds **2R, 4R, and 7R** at 72h showed IC$_{50}$ values of **175 ± 15.53 nM, 179 ± 7.52 nM, and 180 ± 15.00 nM**, respectively. These values are comparable to the IC$_{50}$ of the standard drug Lenvatinib**,** which was found to be **179 ± 7.02 nM** (as presented in Table 6). The corresponding cell viability for compounds 2R, 4R, and 7R was observed to be **86.8 %, 88.9 %, and 87.1** %, respectively, which further supports their potent anti-breast cancer activity. The compounds were comparably superior to the standard Lenvatinib. Furthermore, among the synthesized substituted 1, 3, 4-oxadiazole derivatives, compounds bearing electron-withdrawing groups on the benzene ring exhibited strong anti-cancer activity**.** In contrast, derivatives with electron-donating groups at the same position demonstrated reduced activity**,** which may be attributed to steric hindrance interfering with effective interaction at the biological target site.

CONCLUSION

The 1, 3, 4-oxadiazole core is an important pharmacophore in the development of new anti-breast cancer drugs, according to the study. The biological activity was much increased by the addition of electron-withdrawing groups to the aromatic ring. This was probably because the VEGFR active site had better molecular interactions and binding affinity. Conversely, electron-donating substituents at comparable locations decreased activity, presumably as a result of undesirable electronic or steric consequences. This confirms that adjusting the electronic properties surrounding the pharmacophore can result in powerful and specific anti-cancer agents that target VEGFR. This approach provides a practical way to rationally create and optimize medications for the treatment of breast cancer.

Table 1: Physical properties of synthesized compounds

Sl.no	Compound Code	Molecular Formula	Molecular Weight	MP (^{0}C)	% Yeild	Rf	Mobile phase

1	1R	$C_{20}H_{16}N_2O_4$	348.35	175-177	85	0.43	B:A 9:1
2	2R	$C_{20}H_{14}N_2O_4Cl_2$	417.24	188-190	63	0.24	B:A 9:1
3	3R	$C_{20}H_{17}N_2O_6$	380.35	189-192	61	0.46	B:A 9:1
4	4R	$C_{20}H_{16}N_2O_5$	393.35	184-186	58	0.40	B:A 9:1
5	5R	$C_{20}H_{15}N_3O_6$	364.35	183-186	72	0.34	B:A 9:1
6	6R	$C_{22}H_{20}N_2O_6$	382.8	200-203	60	0.50	B:A 9:1
7	7R	$C_{20}H_{15}N_3O_6$	393.35	162-165	50	0.28	B:A 9:1
8	8R	$C_{20}H_{16}N_2O_5$	364.35	170-172	54	0.34	B:A 9:1
9	9R	$C_{20}H_{16}N_2O_5$	408.4	176-78	56	0.40	B:A 9:1
10	10R	$C_{20}H_{15}N_2O_4Cl$	364.35	180-181	71	0.36	B:A 9:1

B = Benzene A = Acetone

Table 2: Predicted Mole inspiration data of synthesized compounds

Sl.no	Compound code	GPCR ligand	Ionchannel modulator	Kinase inhibitor	Nuclear receptor ligand
1	1R	-0.16	-0.06	-0.11	-0.94
2	2R	-0.17	0.02	-0.19	-1.00
3	3R	-0.19	-0.08	-0.13	-0.98
4	4R	-0.18	-0.07	-0.04	-0.81
5	5R	-0.09	-0.04	-0.11	-0.75
6	6R	-0.03	0.08	0.02	-0.76
7	7R	-0.19	-0.05	0.02	-0.92
8	8R	-0.16	-0.03	-0.20	-0.83
9	9R	-0.14	-0.07	-0.18	-0.92
10	10R	-0.12	-0.09	-0.10	-0.86

Table 3: Infrared spectral study of the synthesized compounds

Compound code	Molecular nature and Spectral peaks (cm^{-1})
1R	2929 (Ar CH Str), 1714 (C=O, lactone), 1616 (C=O, ester), 1247 (C-O, coumarin), 756 (Ar CH Bend).
2R	3065(Ar CH str), 1681(C=O, lactone), 1618 (C=O, ketone), 1186 (C Cl, aromatic), 1572(C=N), 1267 (C-O, coumarin) and 752 (Ar CH bend).
3R	2916 (Ar CH Str.), 1691 (C=O, lactone), 1618 (C=O, ketone), 1525 (C=N), 1346 (C-NO2), 1197 (C-O, coumarin) and 763 (Ar CH Bend).
4R	3012 (Ar CH Str.), 1768 (C=O, lactone), 1616 (C=O, ketone), 1531 (C=N), 1369(C-NO2), 1280 (C-O-C) [oxadiazole nucleus], 1199 (C-O, coumarin), 763 (Ar CH Str).
5R	3065(Ar CH str), 1681(C=O, lactone), 1618 (C=O, ketone), 1186 (C Cl, aromatic), 1572(C=N), 1267 (C-O, coumarin) and 752 (Ar CH bend).
6R	3065(Ar CH str), 1681(C=O, lactone), 1618(C=O, ketone), 1186(C-F, aromatic), 1572(C=N), 1267 (C-O, coumarin) and 752 (Ar CH bend).
7R	3065(Ar CH str), 2860 (CH str, aromatic), 1681(C=O, lactone), 1618(C=O, ketone), 1572 (C=N), 1267 (C-O, coumarin) and 752 (Ar CH bend).
8R	3550(Ar CH str), 2860(C-H str, aromatic), 1681(C=O, lactone), 1618(C=O, ketone), 1572 (C=N), 1267 (C-O, coumarin) and 752 (Ar CH bend).
9R	3382 (NH$_2$), 2929(Ar CH), 1617 (C=O, lactone), 1572 (C=O, ketone),1196 (C-O, coumarin), 754 (Ar CH).

10R	3065(Ar CH str), 1681(C=O, lactone), 1618 (C=O, ketone), 1186 (C Cl, aromatic), 1572(C=N), 1267 (C-O, coumarin) and 752 (Ar CH bend).

Table 4: ^{1}H NMR Spectral data of synthesized compounds

Compound code	Chemical shift value and Proton nature
2R	(400MHz; DMSO d6/TMS, ppm):1.42(3H, t, CH3), 4.44(2H, q, CH2), 7.27-7.69(4H, m, Ar-H), 8.53 (1H, s, Ar-H).
4R	(400MHz; DMSO d6/TMS, ppm):2.38 (3H,s,COCH3),7.32-7.53 (4H,m,Ar-H),7.8 (2H, d, Ar-H),8.11(2H,d, Ar-H),8.6(1H, s, Ar-H),8.7(1H,s, CH of oxadiazole).
7R	(400MHz; DMSO d6/TMS, ppm):2.38 (3H, s, CH₃), 7.15 (4H, m, Ar-H), 7.32(3H,s, CH₃), 7.44 (1H, s, Ar-H), 7.9 (2H, d, Ar-H), 8.11 (2H, d, Ar-H)

Table 5: ADME and Drug Likeness Parameters of synthesized compounds

CC	SA	GI	BBB	PgP	MW	BS	N HBA	N HBD	TPSA	LogP	nLV
1R	4.19	High	Y	N	348.35	0.55	5	0	72.11	3.18	0
2R	4.22	High	Y	N	417.24	0.55	5	0	72.11	3.59	0
3R	4.23	High	N	N	380.35	0.55	7	2	112.57	2.8	0
4R	4.21	High	N	N	393.35	0.55	7	0	117.93	2.93	0
5R	4.18	High	N	N	364.35	0.55	6	1	92.34	2.75	0
6R	4.16	High	Y	N	382.8	0.55	5	0	72.11	3.51	0
7R	4.21	High	N	N	393.35	0.55	7	0	117.93	2.87	0
8R	4.19	High	N	N	364.35	0.55	6	1	92.34	2.78	0
9R	4.42	High	N	N	408.4	0.55	7	0	90.57	3.65	0
10R	4.19	High	N	N	364.35	0.55	6	1	92.34	3.08	0

SA synthetic accessibility, GI gastrointestinal absorption, BBB blood–brain barrier permeant, PgPP-glycoprotein substrate, MW molecular weight, nHBD number of hydrogen bond donor, nHBA number of H-bond acceptor, BS Bio-availability Score, TPSA topological polar surface area, LOG P water partition co-efficient, nLV number of Lipinski violation.

Table 6: Docking results of substituted 1, 3, 4-oxadiazole derivatives

Sl.no	Compound Code	Docking score	Amino acid residue
1	**1R**	-9.1	GLU-885,ILE-888,ASP-1046,LEU-889,VAL-899,CYS-1045, LYS-868
2	**2R**	-9.5	GLU-885, ASP-1046, LEU-1019, ARG-1027, HIS-1026
3	**3R**	-8.8	GLU-885, LEU-1019, ARG-1027
4	**4R**	-9.2	GLU-885, LEU-1019, ARG-1027, GlY-1048
5	**5R**	-8.9	GLU-885, ILE-888, ASP-1046, GLY-1048, LEU-1049, LYS-868
6	**6R**	-9.1	GLU-885, ASP-1046, LEU-1019, LEU-889
7	**7R**	-9.2	GLU-885, LEU-889, LEU-1049, LEU-1019, ILE-888, ALA-881
8	**8R**	-8.9	GLU-885, LEU-1049, LEU-1019, ILE-888, ALA-881, ASP-1046
9	**9R**	-8.6	GLU-885, LEU-1049, LEU-1019, LYS-868 , ASP-1046, ARG-1027,HIS-1026
10	**10R**	-8.9	GLU-885,LEU-1019, ILE-888, ALA-88 ASP-1046
11	Lenvatinib	-7.7	GLU-885, LEU-889, LEU-1049, LEU-1019, ILE-888, ALA-881

Table 7: Cytotoxic effect and cell viability of **2R, 4R & 7R** was readably determined against diseased MCF-7 Cell Lines by MTT assay, time 72h.

Sl.no	Compound Code	IC50±SEM(nm)
1	**2R**	175±15.53
2	**4R**	175±15.53
3	**7R**	179±7.52
4	**Lenvatinib**	180±15

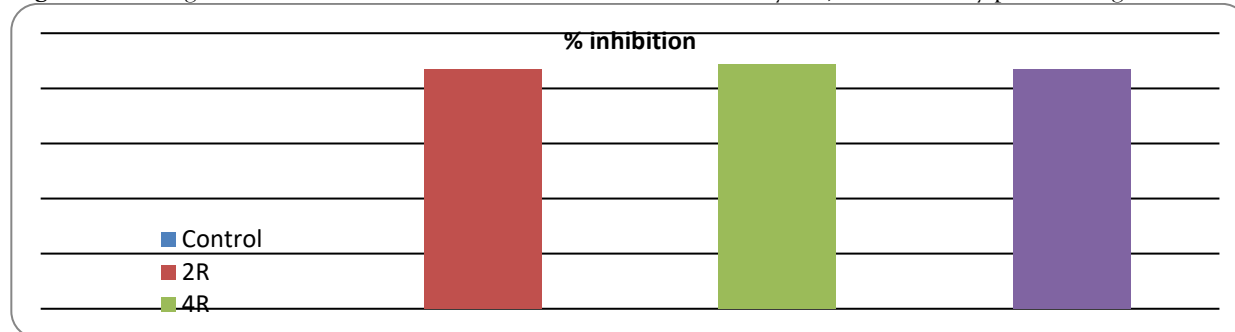**Fig 2:** Percentage of breast cancer cell line MCF-7 that inhibited by **2R, 4R & 7R** by performing MTT Assay
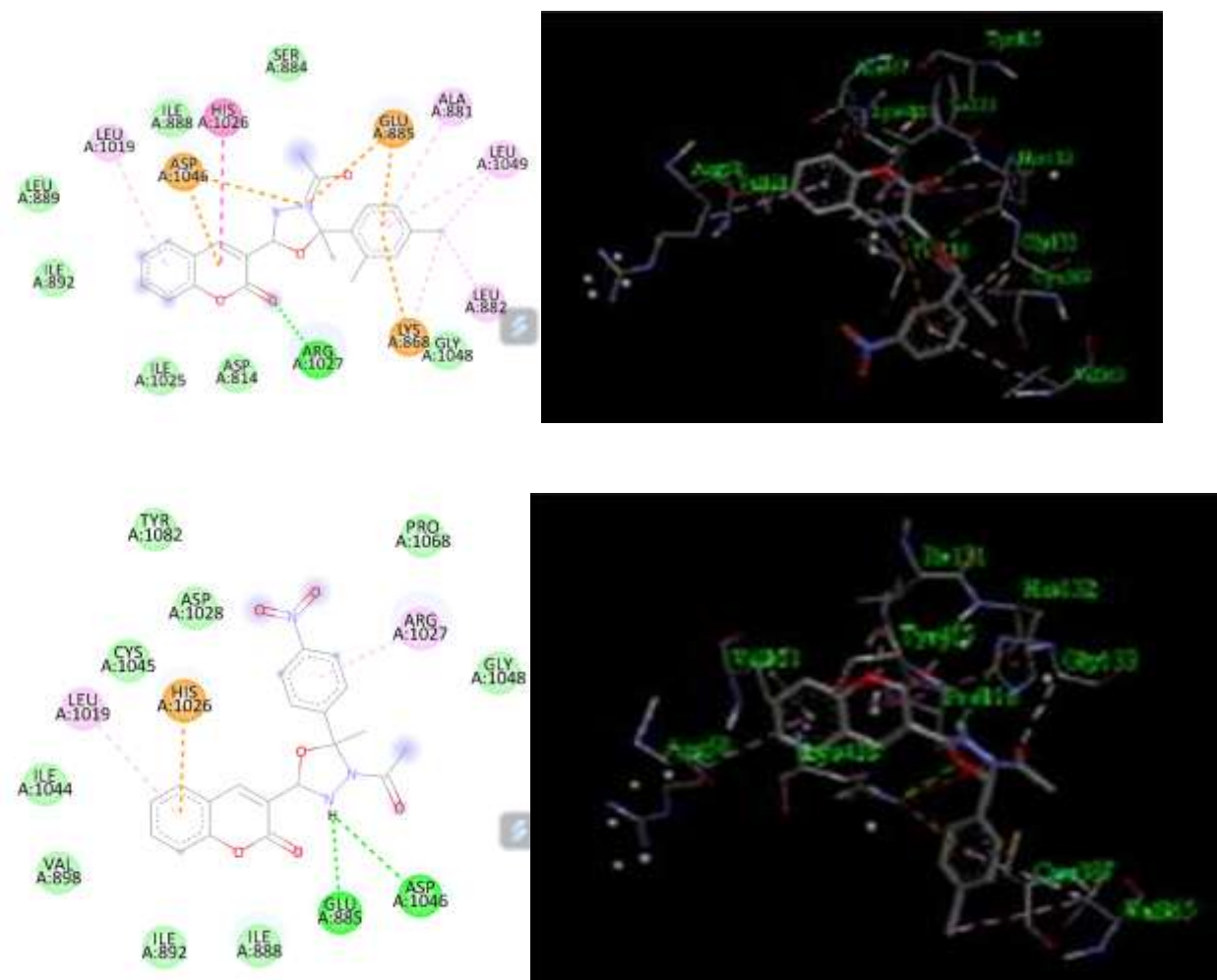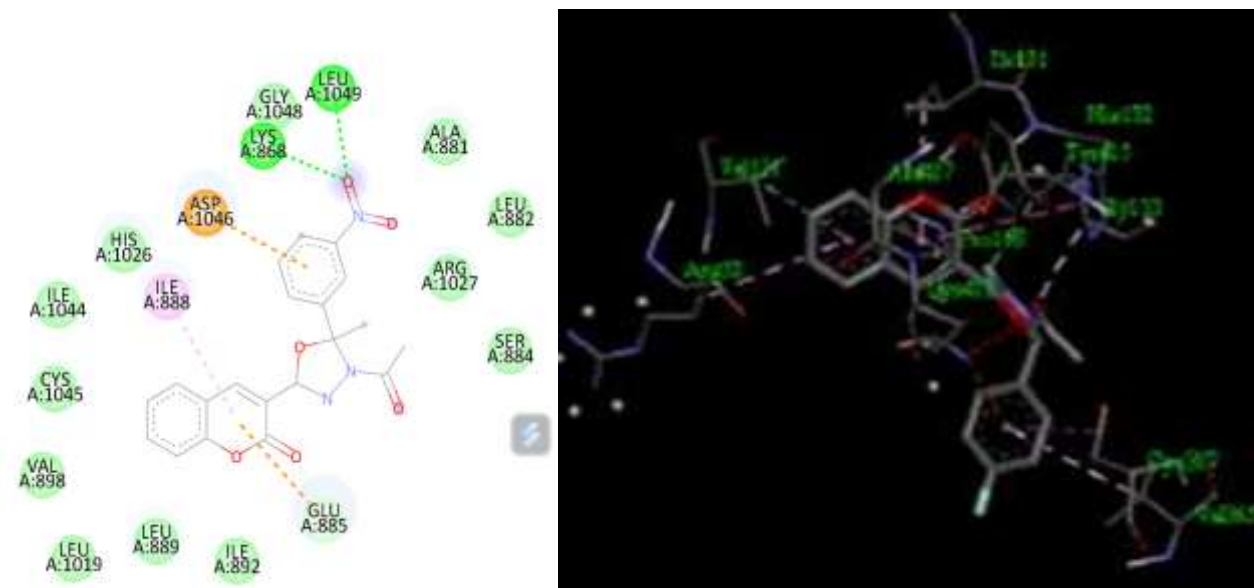

Figure 3: The docking pose of compounds **2R, 4R and 7R** with **VEGFR (3VHK)** respectively.

REFERENCES :

1. Ahmedah HT, Basheer HA, Almazari I, Amawi KF.Introduction to nutrition and cancer. Cancer Treat Res. 2024; 191:1–32. Doi: 10.1007/978-3-031-55622-7

2. Ahsan MJ. 1,3,4-Oxadiazole containing compounds as therapeutic targets for cancer therapy. Mini Rev Med Chem. 2022; 22(1):164–197. Doi: 10.2174/1389557521666210226145837.

3. Niti Bhardwaj S, Saraf K, Pankaj S and Pradeep K. Synthesis, evaluation and characterization of some 1, 3, 4-oxadiazoles as antimicrobial agents. E-Journal of Chemistry.2009; 6(4): 1133-38.

4. Kucukguzel SG, Oruc EE, Rollas S, Sahin F and Ozbek A. Synthesis, characterization and biological activity of novel 4-thiazolidinones, 1,3,4- oxadiazoles and some related compounds. Eur. J. Med. Chem. 2002; 37(3): 197-206.

5. Preethi R Kagthara, Niraj S Shah, Rajeev K Doshi and Parekh H.H. Synthesis of 2,5-disubstituted-1,3,4-oxadiazoles as biologically active heterocycles. Indian.J.Chem. 1999; 38B: 572-76.

6. Narayan Deshpande, Rao YV, Kandlikar RP, Devender AR & Reddy VM.A study of anticonvulsant activity with 6, 8-dibromo 3-(5- aryl-1, 3, 4-oxadlazol-2yl)-methyl)-2-methyl-4(3h) quinazolinones. Indian J. Pharmac.1986; 78: 127-28.

7. Mohd Amir, Javed SA and Harish Kumar.Synthesis of some 1, 3, 4-oxadiazole derivatives as potential anti-inflammatory agents. Indian J. Chem. 2007; 46B: 1014-19.

8. Vasanth Kumar N and Uday C Mashelkar. Synthesis of 1, 2, 4-oxadiazole and biological activities such as analgesics, anti-inflammatory, antimicrobial, antiviral, pesticides and insecticides.Indian J .chem.2007; 46B:216-20.

9.Kalpesh P, Jayachandran E, Ravishsh, Vijaya J and Sreenivasa GM. Synthesis, characterization and Anthelmintic activity of new oxadiazole incorporated with imidazole and pyrazole. Int J of Pharma and Bio Sciences.2010; 1 (3): 1-13.

10. Zachary I. VEGF signalling: integration and multi-tasking in endothelial cell biology. Biochem Soc Trans. 2003; 31(pt 6):1171–1177. doi: 10.1042/bst0311171.

11. Simons M, Gordon E, Claesson-Welsh L. Mechanisms and regulation of endothelial VEGF receptor signalling. Nat Rev Mol Cell Biol.2016; 17: 611–625. doi: 10.1038/nrm.2016.87.4.

12. Simons M. An inside view: VEGF receptor trafficking and signaling.Physiology (Bethesda). 2012; 27: 213–222 doi: 10.1152/physiol.00016.2012.5.

13. Boeldt DS, Yi FX, Bird IM. eNOS activation and NO function: pregnancy adaptive programming of capacitative entry responses alters nitric oxide (NO) output in vascular endothelium–new insights into eNOS regulation through adaptive cell signaling. J Endocrinol. 2011;210:243–258 doi: 10.1530/JOE-11-0053.6.

14. Wang Y, Zang QS, Liu Z, Wu Q, Maass D, Dulan G, Shaul PW, Melito L, Frantz DE, Kilgore JA, Williams NS, Terada LS, Nwariaku FE.Regulation of VEGF-induced endothelial cell migration by mitochondrial reactive oxygen species. Am J Physiol Cell Physiol. 2011; 301:C695–C704. doi: 10.1152/ajpcell.00322.2010.

15. Cabanillas, M.E.; Habra, M.A. Lenvatinib: Role in thyroid cancer and other solid tumors.Cancer Treat. Rev.2016; 42: 47–55.

16. Adeniji SE, Shallangwa GA, Arthur DE, Abdullahi M, Mahmoud AY, Haruna A. Quantum modelling and molecular docking evaluation of some selected quinoline derivatives as antitubercular agents. Heliyon.2020; 1(2): 1010-1020.

17. Iwata H, Oki H, Okada K, Takagi T, Tawada M, et.al.Crystal structure of the VEGFR2 kinase domain in complex with a back pocket binder.2011-08-25 https://doi.org/10.2210/pdb3VHK/pdb.

18. Maria Kontoyianni. Docking and virtual screening in drug discovery,Meth in molec bio. 2017; 1647: 255-266.

19. Madhavi SG, Matvey A, Tyler D, Ramakrishna A, Woody S. Protein and ligand preparation: parameters, protocols, and influence on

virtual screening enrichments. J of Computer-Aided Mol Des.2013; 27: 221–234.

20. Azzam RA, Osman RR, Elgemeie GH. Efficient synthesis and docking studies of novel benzothiazole-based pyrimidine sulfonamide scaffolds as new antiviral agents and HSP90α inhibitors.ACS Omega.2020; 5(3): 1640–55.

21. Kenny L, Shania RAS, Brian WG, Forbes A, Apriliana CK et.al. Anti-Breast Cancer Activity on MCF-7 Cells of Melittin from Indonesia's Apis cerana: An In Vitro Study. Asian Pac J Cancer Prev. 2021; 22(12):3913–3919. doi: 10.31557/APJCP.2021.22.12.3913

22. Horning EC, Horning MG, and Dimmig DA.3-carbethoxy coumarin. Organic Syntheses, 1955; 3: 165.

23. Shashikant PR, Rabara PA, Jayashri PS, Bukitagar AA, Wakale VS and Musumade DS. Synthesis of some novel substituted 1,3,4-oxadiazole and pyrazole derivatives for pyrazole derivatives for antitubercular activity. Indian J.Chem.2009; 48: 1453-56.

24. Siddappa K, Mallikarjun K, Tukaram Reddy, Mallikarjun M, Reddy CV and Mahesh T. Synthesis, characterization and antimicrobial studies of n1-[(1e)-1-(2-hydroxyphenyl) ethylidene]-2-oxo-2h-chromene-3-carbohydrazide and its metal complexes.E-Journal of Chem.2009; 6(3): 615-24.

25. Mashooq AB, Nadeem S and Suroor AK. Synthesis of novel 3-(4- acetyl-5H/ methyl-5-substituted phenyl-4, 5-dihydro-1, 3, 4-oxadiazol-2-yl)- 2H-chromen-2-ones as potential anticonvulsant agents. Acta Poloniae Pharmaceutica-Drug Res.2008; 65: 235-39.

26. Bashmail, H. A.; Alamoudi, A. A.; Noorwali, A.; Hegazy, G. A.; Ajabnoor, G. M.; Al-Abd, A. M. Thymoquinone enhances paclitaxel anti-breast cancer activity via inhibiting tumor-associated stem cells despite apparent mathematical antagonism. Molecules 2020, 25, 426, DOI: 10.3390/molecules25020426

27. Stockert JC, Castro AB, Cañete M , Horobin RB, Villanueva A. MTT assay for cell viability: Intracellular localization of the formazan product is in lipid droplets. Acta histochemica.2012; 8(114): 785-796.

28, Rekha S, Kalpana D, Chandrashekhar S, Sagar DLN, Vedika N et.al. In-silico drug design and ADME studies of substituted 1, 3, 4-oxadiazole analogues as potent mycobacterial DPRE1 enzyme inhibitors..